Oceanology, Vol. 44, No. 4, 2004, pp. 461–471. Translated from Okeanologiya, Vol. 44, No. 4, 2004, pp. 495–506.

MARINE PHYSICS

Nonhydrostatic Model of Marine Circulation

V. B. Zalesnyi[1], R. Tamsalu[2], and T. Kullas[2]

[1]*Institute of Numerical Mathematics, Russian Academy of Sciences, Moscow, Russia*
[2]*Estonian Marine Institute, Tallinn, Estonia*

Received October 8, 2003

Abstract—A nonhydrostatic σ-model of marine dynamics is presented. A numerical algorithm for solving the problem based on the method of splitting with respect to the physical processes and geometric coordinates is described. The splitting method allows the construction of an efficient numerical model, which is a natural improvement of the input model based on the primitive equations. The model is tested in a series of calculations of marine dynamics in a rectangular sea (academic) basin. The academic basin approximates the middle part of the Baltic Sea. The results of numerical calculations for different (low and high) horizontal resolutions of the model in the hydrostatic and nonhydrostatic approximations are described. To illustrate the model adequacy, the results of the calculation of the Gulf of Finland dynamics are presented.

INTRODUCTION

The results of numerical modeling of sea and ocean dynamics indicate that the best way to improve the models is to enhance their spatial resolution [8, 10]. The enhancement of the spatial resolution of the models requires, as a rule, their physical content to be enriched. For example, with the decrease in the horizontal mesh size, when the horizontal mesh size approaches the vertical mesh size, the condition that the vertical scale is small with respect to the horizontal scale will not be satisfied. This may cause us to give up the hydrostatic approximation and to consider the complete equation for the vertical velocity.

In addition, recently, marine processes have more often been analyzed and predicted by performing series of numerical calculations within a set of diminishing embedded subdomains. This way to a more detailed description of the processes studied makes the horizontal and vertical scales approach each other. Embedding of the calculation domains results in "embedding" calculation models and stimulates the development of a hierarchy of models, which allows us to use models of different levels of physical complexity while remaining under the auspices of a single algorithm.

Our study is devoted to the construction of such a hierarchic nonhydrostatic model of marine dynamics. The principal requirement is that the model should be able to resolve the physical problems of different levels of complexity. The hierarchic structure of the model is based on the method of splitting with respect to physical processes [4, 14, 15]. The model is an improvement of the model based on the equations of the general circulation in the ocean (primitive equations) written in the spherical σ-coordinate system [15]. The model was improved in two directions. First, account for the nonhydrostatic effect, and, second, "$k - \epsilon$" parametrization of the processes of turbulent exchange were applied. Since the input model is based on the splitting method, its program realization is modular. Individual splitting stages are represented by individual program units. The principal improvement of the model—the allowance for the nonhydrostatic effect—was achieved by adding a complementary splitting stage to the input model. The program package was provided with a new unit for the calculation of the nonhydrostatic dynamics, with the base of the model kept unchangeable. We managed to achieve this owing to the equivalent transformation of the initial equations of motion. The transformation needs a new function to be introduced, a function describing pressure variations. This technique is similar to the representation of pressure as a sum of the hydrostatic and nonhydrostatic components, which was used in [12].

In this paper, we present the formulation of the nonhydrostatic σ-model and the method of its numerical solution. The model is used for the calculations of the thermohaline marine dynamics within an ideal rectangular area, conventionally called an "academic basin," which simulates the conditions in the central Baltic Sea. The main goal of the numerical experiments was to approbate the nonhydrostatic model and to assess the nonhydrostatic effect under such ideal conditions. In addition, to illustrate the adequacy of the model, we present the results of the calculations of the dynamics of the Gulf of Finland.

MODEL EQUATIONS

The nonhydrostatic model of the thermohaline dynamics is based on a system of nonlinear three-dimensional equations. The model includes:

—complete nonlinear equations of motion for the velocity vector with the components u, v, and w written in the Boussinesq approximation;

—a three-dimensional equation of transfer–diffusion for the potential temperature T;

—a three-dimensional equation of transfer–diffusion for the salinity S;

—three-dimensional equations of transfer–diffusion–kinetics for the turbulent kinetic energy κ and its dissipation rate ε;

—a continuity equation for an incompressible fluid;

—an equation of state for seawater.

The equations written in the spherical σ-coordinate system ($\sigma = z/H(\lambda, \varphi)$) have the form [12, 15]

$$\frac{du}{dt} - \hat{l}v + m\left(\frac{n}{m}\right)'uv + nwu + \tilde{l}w = -\frac{m}{\rho_0}\left(\frac{\partial p}{\partial \lambda} - \frac{\sigma}{H}\frac{\partial H}{\partial \lambda}\frac{\partial p}{\partial \sigma}\right) + \Lambda u, \quad (1)$$

$$\frac{dv}{dt} + \hat{l}u - m\left(\frac{n}{m}\right)'uu + nwv = -\frac{n}{\rho_0}\left(\frac{\partial p}{\partial \theta} - \frac{\sigma}{H}\frac{\partial H}{\partial \theta}\frac{\partial p}{\partial \sigma}\right) + \Lambda v, \quad (2)$$

$$\frac{dw}{dt} - \tilde{l}u - n(u^2 + v^2) = -\frac{1}{\rho_0 H}\left(\frac{\partial p}{\partial \sigma} - gH\rho\right) + \Lambda w, \quad (3)$$

$$m\left[\frac{\partial uH}{\partial \lambda} + \frac{\partial}{\partial \theta}\left(\frac{n}{m}vH\right)\right] + \frac{\partial w_*}{\partial \sigma} = \frac{\partial \zeta}{\partial t}, \quad (4)$$

$$\frac{dT}{dt} = \Lambda T, \quad (5)$$

$$\frac{dS}{dt} = \Lambda S, \quad (6)$$

$$\frac{d\kappa}{dt} = \gamma_1\frac{\kappa^2}{\varepsilon} - \varepsilon + \Lambda\kappa, \quad (7)$$

$$\frac{d\varepsilon}{dt} = c_1\gamma_2\kappa - c_2\frac{\varepsilon^2}{\kappa} + \Lambda\varepsilon, \quad (8)$$

$$\rho = f(T, S, p). \quad (9)$$

Here

$$\frac{d*}{dt} = \frac{1}{H}\left[\frac{\partial}{\partial t}H* + m\left(\frac{\partial}{\partial \lambda}Hu* + \frac{\partial}{\partial \theta}\frac{n}{m}Hv*\right) + \frac{\partial}{\partial \sigma}w_**\right], \quad (10)$$

$$w_* = w - \sigma\left(um\frac{\partial H}{\partial \lambda} + vn\frac{\partial H}{\partial \theta}\right) - (1 - \sigma)\frac{\partial \zeta}{\partial t}, \quad (11)$$

$$\Lambda* = (\Lambda_\lambda + \Lambda_\theta + \Lambda_\sigma)*, \quad (12)$$

$$\Lambda_\lambda* = \frac{1}{H}m^2\left[\frac{\partial}{\partial \lambda}\mu_*H\frac{\partial*}{\partial \lambda} - \frac{\partial}{\partial \lambda}\left(\mu_*\sigma\frac{\partial H}{\partial \lambda}\frac{\partial*}{\partial \sigma}\right) - \frac{\partial}{\partial \sigma}\left(\mu_*\sigma\frac{\partial H}{\partial \lambda}\frac{\partial*}{\partial \lambda}\right) + \frac{\partial}{\partial \sigma}\left(\mu_*\frac{\sigma^2H_\lambda^2}{H}\frac{\partial*}{\partial \sigma}\right)\right], \quad (13)$$

$$\Lambda_\theta* = \frac{1}{H}mn\left[\frac{\partial}{\partial \theta}\mu_*Hq\frac{\partial*}{\partial \theta} - \frac{\partial}{\partial \theta}\left(\mu_*\sigma q\frac{\partial H}{\partial \theta}\frac{\partial*}{\partial \sigma}\right) - \frac{\partial}{\partial \sigma}\left(\mu_*\sigma q\frac{\partial H}{\partial \theta}\frac{\partial*}{\partial \theta}\right) + \frac{\partial}{\partial \sigma}\left(\mu_*\frac{\sigma^2H_\theta^2q}{H}\frac{\partial*}{\partial \sigma}\right)\right], \quad (14)$$

$$\Lambda_\sigma* = \frac{1}{H^2}\frac{\partial}{\partial \sigma}\nu\frac{\partial*}{\partial \sigma}, \quad (15)$$

$$\gamma_1 = \frac{c_\mu}{H^2}\left[\left(\frac{\partial u}{\partial \sigma}\right)^2 + \left(\frac{\partial v}{\partial \sigma}\right)^2 - \frac{H}{\sigma_T}\frac{\partial b}{\partial \sigma}\right], \quad (16)$$

$$\gamma_2 = \frac{c_\mu}{H^2}\left[\left(\frac{\partial u}{\partial \sigma}\right)^2 + \left(\frac{\partial v}{\partial \sigma}\right)^2 - c_3\frac{H}{\sigma_T}\frac{\partial b}{\partial \sigma}\right], \quad (17)$$

where λ is the longitude; $\theta = 90° + \psi$; ψ is the latitude; σ is the vertical coordinate pointed downward; ζ is the sea level (its positive value denotes a depression and its negative one denotes a rise); $H(\lambda, \theta)$ is the sea depth; $\nu_* = c_\mu\kappa^2\varepsilon^{-1}$ is the coefficient of the vertical turbulent exchange; μ_* is the coefficient of the horizontal turbulent exchange; $\hat{l} = -2\Omega\cos\theta$, $\tilde{l} = 2\Omega\sin\theta$, Ω is the angular velocity of the earth's rotation; $m = 1/(R\sin\theta)$, $n = 1/R$ are the metric coefficients; R is the earth's radius; $q = n/m$; p is the pressure; $b = g(\rho - \rho_0)/\rho_0$ is the buoyancy; ρ is the density of seawater; $\rho_0 \equiv$ const is the reference density; g is the acceleration due to gravity; and $\sigma_T = f(\mathrm{Ri})$, where Ri is the Richardson number; and c_μ, c_1, c_2, and c_3 are constants. The process of the turbulent exchange is parameterized with the κ–ε model [6].

The boundary conditions for (1)–(9) are formulated as follows.

Over the vertical line, at the top boundary, for $\sigma = 0$ we have

$$\nu_u\frac{\partial}{\partial \sigma}\begin{pmatrix} u \\ v \end{pmatrix} = -\frac{H}{\rho_0}\begin{pmatrix} \tau_1 \\ \tau_2 \end{pmatrix}; \quad \nu_c\frac{\partial c}{\partial \sigma} = -HQ_c^0; \quad w_* = 0, \quad (18)$$

where c and Q_c are vector-functions represented as

$$c = (T, S, \kappa, \varepsilon)', \quad Q_c = (Q_T, Q_S, Q_\kappa, Q_\varepsilon)'. \quad (19)$$

At the bottom boundary, for $\sigma = 1$

$$\nu_u\frac{\partial}{\partial \sigma}\begin{pmatrix} u \\ v \end{pmatrix} = 0; \quad \nu_c\frac{\partial c}{\partial \sigma} = -HQ_c^1; \quad w_* = 0. \quad (20)$$

At the side surface Σ

$$\mu_*\frac{\partial c}{\partial \hat{n}} = 0; \quad u = v = 0. \quad (21)$$

Here τ_1 and τ_2 are the components of the wind friction tension, Q_T is the heat flux, Q_S is the salinity flux, Q_κ is the turbulent energy flux, Q_ε is the flux of the turbulent energy dissipation rate, and $\hat{n}$ is the vector normal to Σ.

Equations (1)–(9) should be complemented by the initial conditions for $t = 0$

$$U = \begin{pmatrix} u \\ v \end{pmatrix} = U^0; \quad c = c^0. \tag{22}$$

Note 1. Besides the initial vertical velocity w, the new vertical velocity w_* is used in the new coordinate system. It is equal to zero at the sea surface, $\sigma = 0$, and at the bottom, $\sigma = 1$, since the kinematic conditions for w

$$w = \frac{\partial \zeta}{\partial t} \quad \text{at} \quad z = 0, \tag{23}$$

$$w = um\frac{\partial H}{\partial \lambda} + vn\frac{\partial H}{\partial \theta} \quad \text{at} \quad z = H(\lambda, \theta) \tag{24}$$

are satisfied.

The new vertical velocity w_* is associated with the form of the transport operator in the σ-coordinate system, in which it has the form

$$\frac{d}{dt} = \frac{\partial}{\partial t} + mu\frac{\partial}{\partial \lambda} + nv\frac{\partial}{\partial \theta} + [w - (mZ_\lambda u + nZ_\theta v + Z_t)]\frac{\partial}{\partial \sigma}, \tag{25}$$

$$Z = \sigma(H - \zeta) + \zeta. \tag{26}$$

Neglecting the spatial gradients ζ in comparison to the gradients H we have

$$Z_\lambda = \sigma H_\lambda, \quad Z_\theta = \sigma H_\theta, \quad Z_t = (1 - \sigma)\zeta_t. \tag{27}$$

Note 2. The continuity equation can be rewritten in terms of the old vertical velocity

$$m\left[\frac{\partial uH}{\partial \lambda} + \frac{\partial}{\partial \theta}\left(\frac{n}{m}vH\right)\right] + \frac{\partial w}{\partial \sigma} - \frac{\partial}{\partial \sigma}[\sigma(mH_\lambda u + nH_\theta v)] = 0. \tag{28}$$

SPLITTING METHOD

To solve Eqs. (1)–(9) with respect to time, let us use the splitting method. The mathematical aspects of the splitting method and its use for the solution of oceanological problems are presented in [1, 2, 4, 14]. The essence of the method is as follows. Let us assess a nonstationary problem

$$\frac{\partial \varphi}{\partial t} + A\varphi = 0, \quad \varphi = (u, v, w, T, S, \kappa, \varepsilon)', \tag{29}$$

where A is the nonnegative operator which can be presented as a superposition of simpler operators A_i

$$A = \sum_{i=1}^{N} A_i, \quad A_i \geq 0. \tag{30}$$

Then, for solving (29), we can use the implicit splitting scheme

$$\begin{aligned} \bar{\varphi} &= \bar{\varphi}^j + \tau f^j, \\ (E + \tau A_1)\varphi^{j+1/n} &= \bar{\varphi}, \\ (E + \tau A_2)\varphi^{j+2/n} &= \varphi^{j+1/n}, \\ &\cdots \\ (E + \tau A_N)\varphi^{j+1} &= \varphi^{j+(N-1)/N}. \end{aligned} \tag{31}$$

The scheme (31) is absolutely stable and approximates (29) to the first-order accuracy in time.

The splitting method can be considered not only as an efficient method for solving a complex problem in time but as the basis for the construction of a hierarchic model system. Within the frameworks of a single approach, we can formulate a particular model of ocean dynamics of different complexity from the point of view of physical completeness, dimensionality, and spatial resolution. The key point in the construction of the split hierarchic model system and the method for its solution is the splitting of the initial base problem into simple subproblems with nonnegative operators. The choice of such a splitting is frequently nontrivial and nonunique [5, 9]. The splitting is reduced to the choice of a series of simpler particular problems. For each particular problem, the conservation law should be satisfied.

In splitting, we can separate several levels. The macrolevel of splitting is based on splitting into physical processes. At the lower level, the simplest problems, one-dimensional in space, may be distinguished.

After splitting of a problem at the macrolevel, it may need to be transformed at a particular stage. This may be filtration (simplification) of the equations and regularization, i.e., adding complementary terms which improve the properties and the solution algorithm of the problem. After the regularization of the splitting stages, a question arises about which method of solving should be used at a particular stage. Choosing the spatial approximation method, we should take into account the properties of the particular problem. Different problems may require different methods for their approximation and solution. In our calculations, we used finite difference approximations over a shifted "C" grid [5].

An intrinsic property of the split model is its modular concept: one problem–one module. Each problem/module may have its own conjugated analog. The integrated model can be composed of different numbers of modules. The computation characteristics of the

model can be improved through changing individual computation modules.

To solve our problem, we use splitting with respect to physical processes (the macrolevel of splitting) and to spatial variables (the microlevel of splitting).

Transfer–diffusion of substances. At the first stage of splitting with respect to physical processes, we solve the problem of momentum transfer–diffusion taking into account metric terms, the turbulent diffusion of heat and salinity, as well as transfer–diffusion of the turbulent kinetic energy and its dissipation rate. We have

$$\frac{du}{dt} + m\left(\frac{n}{m}\right)' uv + nwu + \tilde{l}w = \Lambda u, \tag{32}$$

$$\frac{dv}{dt} - m\left(\frac{n}{m}\right)' uu + nwv = \Lambda v, \tag{33}$$

$$\frac{dw}{dt} - \tilde{l}u - n(u^2 + v^2) = \Lambda w, \tag{34}$$

$$\frac{\partial T}{\partial t} = \Lambda T, \tag{35}$$

$$\frac{\partial S}{\partial t} = \Lambda S, \tag{36}$$

$$\frac{d\kappa}{dt} = \Lambda \kappa, \tag{37}$$

$$\frac{d\varepsilon}{dt} = \Lambda \varepsilon. \tag{38}$$

For efficient solving of the three-dimensional transfer–diffusion equations at the microlevel, the problem is split into coordinates λ, θ, σ

$$\left[\frac{\partial}{\partial t} + um\frac{\partial}{\partial \lambda} - \Lambda_\lambda\right]\varphi = 0, \tag{39}$$

$$\left[\frac{\partial}{\partial t} + vn\frac{\partial}{\partial \theta} - \Lambda_\theta\right]\varphi = 0, \tag{40}$$

$$\left[\frac{\partial}{\partial t} + w_*\frac{\partial}{\partial \sigma} - \Lambda_\sigma\right]\varphi = 0. \tag{41}$$

Adaptation of the velocity and potential density fields. At the second stage of the splitting with respect to the physical processes, the stage of the adaptation of the velocity and potential density fields is specified. At this stage, the equations have the form

$$\frac{\partial u}{\partial t} - \hat{l}v + \frac{m}{\rho_0}\left(\underbrace{\frac{\partial p}{\partial \lambda}}_{0} - \underbrace{\frac{\sigma}{H}\frac{\partial H}{\partial \lambda}\frac{\partial p}{\partial \sigma}}_{1}\right) = 0 \tag{42}$$

$$\frac{\partial v}{\partial t} + \hat{l}u + \frac{n}{\rho_0}\left(\underbrace{\frac{\partial p}{\partial \theta}}_{0} - \underbrace{\frac{\sigma}{H}\frac{\partial H}{\partial \theta}\frac{\partial p}{\partial \sigma}}_{2}\right) = 0, \tag{43}$$

$$\frac{\partial w}{\partial t} + \frac{1}{\rho_0 H}\left(\underbrace{\frac{\partial p}{\partial \sigma}}_{0} - \underbrace{gH\rho}_{3}\right) = 0, \tag{44}$$

$$\begin{aligned} &\underbrace{m\left[\frac{\partial uH}{\partial \lambda} + \frac{\partial}{\partial \theta}\left(\frac{n}{m}vH\right)\right]}_{0} + \frac{\partial w}{\partial \sigma} \\ &- \frac{\partial}{\partial \sigma}[\sigma(\underbrace{mH_\lambda u}_{1} + \underbrace{nH_\theta v}_{2}) + (1-\sigma)\zeta_t] = \frac{\partial \zeta}{\partial t}, \end{aligned} \tag{45}$$

$$\begin{aligned} &H\frac{\partial \rho}{\partial t} + \underbrace{\frac{\partial}{\partial \lambda}(mHu\rho)}_{4} + \underbrace{\frac{\partial}{\partial \theta}(nHv\rho)}_{5} \\ &+ \frac{\partial}{\partial \sigma}[\underbrace{w}_{3} - \sigma(\underbrace{mH_\lambda u}_{4} + \underbrace{nH_\theta v}_{5}) - (1-\sigma)\zeta_t]\rho = 0. \end{aligned} \tag{46}$$

Here, instead of the equations for the temperature and salinity transport, an equation for the potential density transport is written. This can be done assuming the potential density to be a smooth function of the potential temperature and salinity. In our model, the UNESCO-80 formula [7] is used as the equation of state for the seawater, so that the assumption made is valid.

Note 3. Let us assume that during the adaptation stage the sea level ζ does not vary in time, so that $\frac{\partial \zeta}{\partial t} = 0$. Then, the scalar product of Eqs. (42)–(46) by the vector $(\rho_0 Hu, \rho_0 Hv, \rho_0 Hw, p, -\sigma gH)$ helps to satisfy the conservation law for the total energy:

$$\int_D \left(H\rho_0 \frac{u^2 + v^2 + w^2}{2} - \sigma g H^2 \rho\right) dD = 0. \tag{47}$$

The pairwise energetically neutral terms in the equations (42)–(46) are denoted by the same numbers. Specifying of such groups of the terms is convenient for the subsequent splitting of the adaptation equation system. The complementary stages of the splitting are specified so that the conservation law is satisfied at every stage, i.e., a combination of pairwise energetically neutral terms should be presented. Thus, we have to split the equation for the vertical velocity w into two parts, calculating the vertical pressure gradient $\frac{\partial p}{\partial \sigma}$ and the term describing the buoyancy effect $gH\rho$ at different stages of the splitting. As a rule, these terms balance each other and there is no reason to calculate them at different stages of the splitting. In order to overcome this difficulty, another approach should be applied: instead of p we introduce the new function $\tilde{p}$.

Let us rewrite the equations for the vertical velocity in an equivalent form

$$\frac{\partial w}{\partial t} + \frac{1}{\rho_0 H}\frac{\partial}{\partial \sigma}\left[p - \left(p_g(0) + \int_0^\sigma gH\rho d\sigma \right)\right] = 0, \quad (48)$$

where $p_g(0)$ is the hydrostatic pressure at the nondisturbed surface $z = 0$

$$p_g(0) = -g\rho_0\zeta, \quad (49)$$

and introduce a new function $\tilde{p}$ which describes the deviation of pressure from the hydrostatic value

$$\tilde{p} = p - \left(p_g(0) + \int_0^\sigma gH\rho d\sigma \right). \quad (50)$$

Denoting

$$p_g = p_g(0) + \int_0^\sigma gH\rho d\sigma, \quad (51)$$

we obtain Eqs. (42)–(46) in the form

$$\frac{\partial u}{\partial t} - \hat{l}v + \frac{m}{\rho_0}\left(\frac{\partial p_g}{\partial \lambda} - g\rho\sigma\frac{\partial H}{\partial \lambda}\right) + \frac{m}{\rho_0}\left(\frac{\partial \tilde{p}}{\partial \lambda} - \frac{1}{H}\frac{\partial p}{\partial \sigma}\sigma\frac{\partial H}{\partial \lambda}\right) = 0, \quad (52)$$

$$\frac{\partial v}{\partial t} + \hat{l}u + \frac{n}{\rho_0}\left(\frac{\partial p_g}{\partial \theta} - g\rho\sigma\frac{\partial H}{\partial \theta}\right) + \frac{n}{\rho_0}\left(\frac{\partial \tilde{p}}{\partial \theta} - \frac{1}{H}\frac{\partial p}{\partial \sigma}\sigma\frac{\partial H}{\partial \theta}\right) = 0, \quad (53)$$

$$\frac{\partial w}{\partial t} + \frac{1}{\rho_0 H}\frac{\partial \tilde{p}}{\partial \sigma} = 0, \quad (54)$$

$$m\left[\frac{\partial uH}{\partial \lambda} + \frac{\partial}{\partial \theta}\left(\frac{n}{m}vH\right)\right] + \frac{\partial w}{\partial \sigma} - \frac{\partial}{\partial \sigma}[\sigma(mH_\lambda u + nH_\theta v)] = 0, \quad (55)$$

$$H\frac{\partial \rho}{\partial t} + \frac{\partial}{\partial \lambda}(mHu\rho) + \frac{\partial}{\partial \theta}(nHv\rho) + \frac{\partial}{\partial \sigma}[w - \sigma(mH_\lambda u + nH_\theta v) - (1-\sigma)\zeta_t]\rho = 0. \quad (56)$$

This system also satisfies the conservation law of the total energy. We can verify it by multiplying the system by the vector $(\rho_0 Hu, \rho_0 Hv, \rho_0 Hw, \tilde{p}, -\sigma gH)$ and taking into account

$$\frac{\partial p_g}{\partial \sigma} = gH\rho. \quad (57)$$

The procedure such as the introduction of a new function describing the pressure variation is similar to the representation of the pressure as a sum of the hydrostatic and nonhydrostatic parts used in [11, 12].

Hydrostatic regime. Once the convenient form of the equations has been chosen, the adaptation equations may be further split into two stages, which describe the hydrostatic and nonhydrostatic regimes. During the hydrostatic stage, we have

$$\frac{\partial u}{\partial t} - \hat{l}v + \frac{m}{\rho_0}\left(\frac{\partial p_g}{\partial \lambda} - g\rho\sigma\frac{\partial H}{\partial \lambda}\right) = 0, \quad (58)$$

$$\frac{\partial v}{\partial t} + \hat{l}u + \frac{n}{\rho_0}\left(\frac{\partial p_g}{\partial \theta} - g\rho\sigma\frac{\partial H}{\partial \theta}\right) = 0, \quad (59)$$

$$\frac{\partial w}{\partial t} = 0, \quad (60)$$

$$m\left[\frac{\partial (u-\bar{u})H}{\partial \lambda} + \frac{\partial}{\partial \theta}\frac{n(v-\bar{v})H}{m}\right] + \frac{\partial w_*}{\partial \sigma} = 0, \quad (61)$$

$$\frac{\partial \zeta}{\partial t} = m\left[\frac{\partial \bar{u}H}{\partial \lambda} + \frac{\partial}{\partial \theta}\left(\frac{n}{m}\bar{v}H\right)\right], \quad (62)$$

$$H\frac{\partial \rho}{\partial t} + \frac{\partial}{\partial \lambda}(mHu\rho) + \frac{\partial}{\partial \theta}(nHv\rho) + \frac{\partial}{\partial \sigma}(w_*\rho) = 0. \quad (63)$$

A method for solution of equations (58)–(63) is presented in [1, 15]. According to this method, the horizontal velocity components u and v are presented as a sum of the values averaged over the vertical and of the deviations from the average. For the calculations of the vertically averaged motion, an implicit scheme is use. At each time step, the problem is reduced to the iteration solution of the elliptic equation for the sea surface level with the oblique derivative as the boundary condition [3].

Nonhydrostatic regime. At the stage of solving the equations of nonhydrostatic dynamics, we have

$$\frac{\partial u}{\partial t} + \frac{m}{\rho_0}\left(\frac{\partial \tilde{p}}{\partial \lambda} - \frac{1}{H}\frac{\partial p}{\partial \sigma}\sigma\frac{\partial H}{\partial \lambda}\right) = 0, \quad (64)$$

$$\frac{\partial v}{\partial t} + \frac{n}{\rho_0}\left(\frac{\partial \tilde{p}}{\partial \theta} - \frac{1}{H}\frac{\partial p}{\partial \sigma}\sigma\frac{\partial H}{\partial \theta}\right) = 0, \quad (65)$$

$$\frac{\partial w}{\partial t} + \frac{1}{\rho_0 H}\frac{\partial \tilde{p}}{\partial \sigma} = 0, \quad (66)$$

$$m\left[\frac{\partial uH}{\partial \lambda} + \frac{\partial}{\partial \theta}\left(\frac{n}{m}vH\right)\right] + \frac{\partial w}{\partial \sigma} - \frac{\partial}{\partial \sigma}[\sigma(mH_\lambda u + nH_\theta v)] = 0, \quad (67)$$

$$H\frac{\partial \rho}{\partial t} = 0. \quad (68)$$

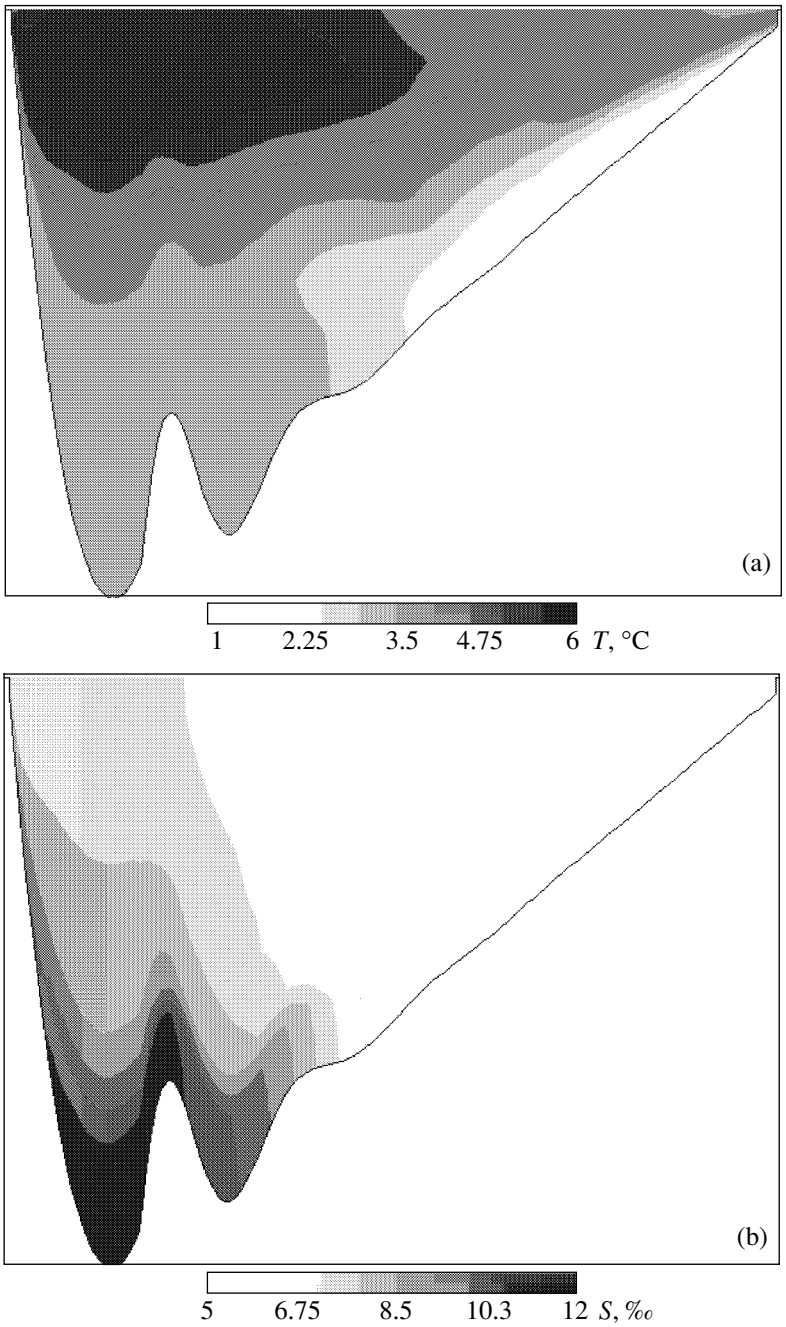

Fig. 1. Distributions of (a) temperature (°C) and (b) salinity (‰) in the vertical latitudinal section in the academic basin on May 9, 1995, at 12:00 AM.

From the point of view of the development of the model of ocean and sea dynamics, this stage is an additional one. Through including it into the model, nonhydrostatic effects are taken into account. It can be easily seen that, if we omit this stage, the model is reduced to its basic formulation—the hydrostatic σ-model of the general circulation.

To approximation the equations at the stage of the calculation of the nonhydrostatic dynamics, we used a semi-explicit time scheme. At the implicit step, we found the terms describing the vertical field structure. The calculation included the solution of the vertically one-dimensional equation of the second order with respect to the pressure and the calculation of the velocity and potential density components from explicit formulas.

Calculation of the turbulent kinetic energy. During this splitting stage, we solve the equations

$$\frac{\partial \kappa}{\partial t} = \gamma_1 \frac{\kappa^2}{\varepsilon} - \varepsilon, \qquad (69)$$

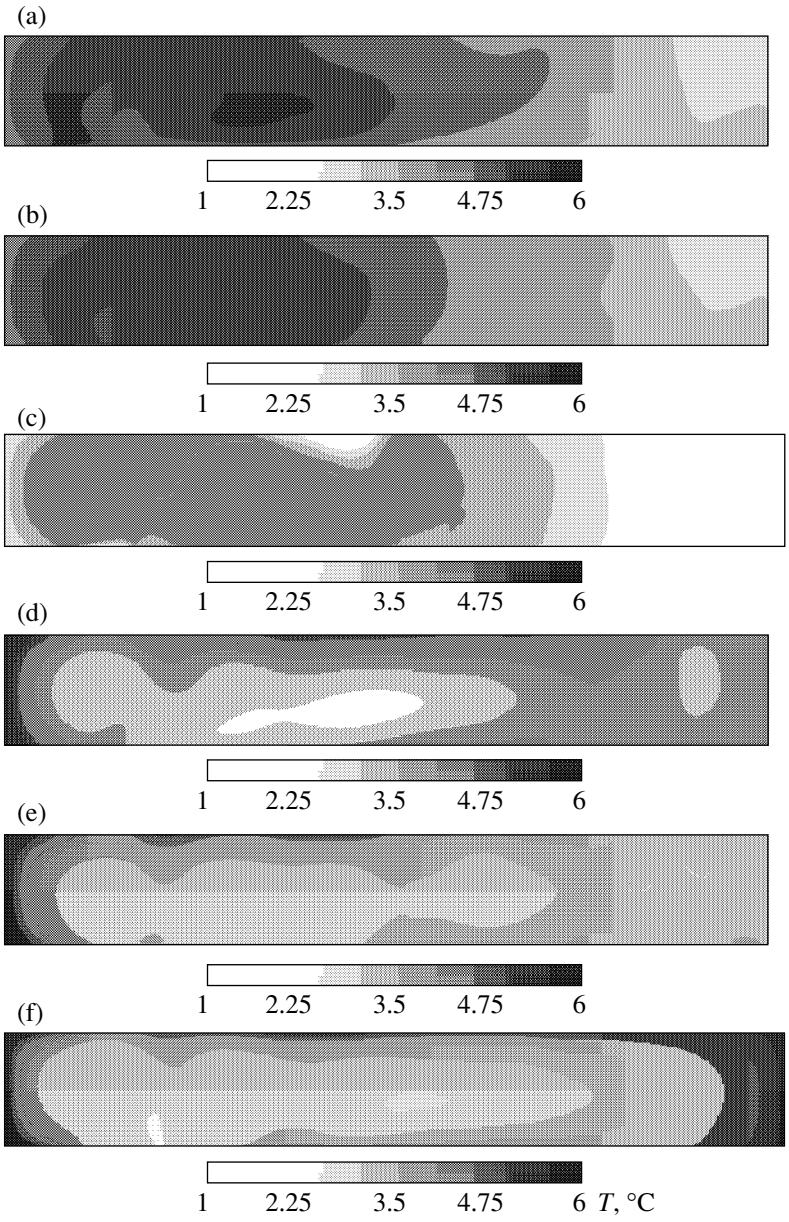

Fig. 2. Temperature (°C) at the surface and at the 8th calculation level in the academic basin on May 9, 1995, at 12:00 AM. (a) Surface, hydrostatic approximation, low resolution; (b) surface, nonhydrostatic approximation, low resolution; (c) surface, nonhydrostatic approximation, high resolution; (d) 8th calculation level, hydrostatic approximation, low resolution; (e) 8th calculation level, nonhydrostatic approximation, low resolution; and (f) 8th calculation level, nonhydrostatic approximation, high resolution.

$$\frac{\partial \varepsilon}{\partial t} = c_1 \gamma_2 \kappa - c_2 \frac{\varepsilon^2}{\kappa}. \quad (70)$$

Using the substitution $X = \kappa/\varepsilon$, Eqs. (69)–(70) can be reduced to the single equation

$$\frac{dX}{dt} + bX^2 = a, \quad (71)$$

where $a = c_1\gamma_2 - \gamma_1$, $b = c_2 - 1 > 0$. For Eq. (71), we can write an analytical solution [6], depending on the initial condition. We use this analytical solution at this stage of splitting.

NUMERICAL EXPERIMENT. ACADEMIC BASIN

The nonhydrostatic model of sea dynamics presented above was approbated in a series of numerical experiments. The first numerical experiment was devoted to testing the model for different input conditions: with and without allowance for the nonhydrostatic effect as well as for high and low spatial resolu-

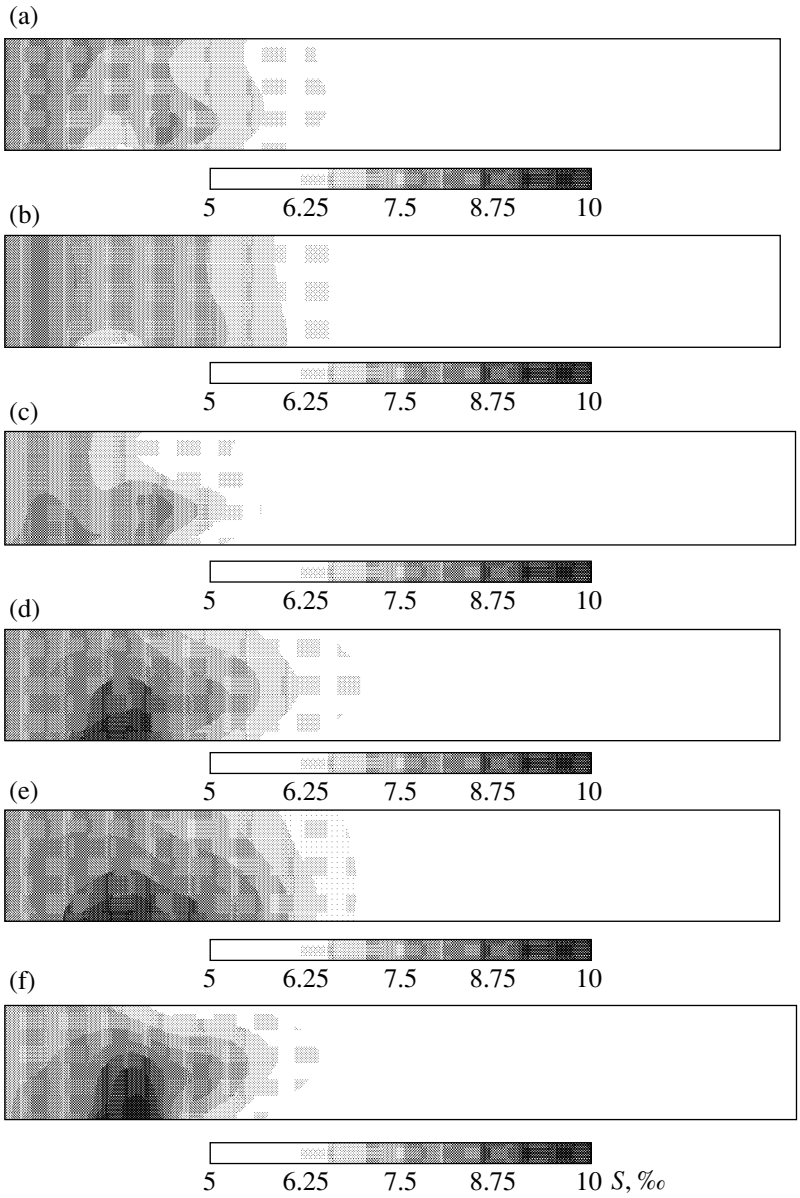

Fig. 3. Salinity (‰) at the surface and at the 8th calculation level in the academic basin on May 9, 1995, at 12:00 AM. (a) Surface, hydrostatic approximation, low resolution; (b) surface, nonhydrostatic approximation, low resolution; (c) surface, nonhydrostatic approximation, high resolution; (d) 8th calculation level, hydrostatic approximation, low resolution; (e) 8th calculation level, nonhydrostatic approximation, low resolution; and (f) 8th calculation level, nonhydrostatic approximation, high resolution.

tion. The numerical experiment was carried out in a simple rectangular calculation domain (academic basin)

The academic basin approximated the northern Baltic Sea located at the latitudes of the Gulf of Finland from the coast of Sweden to the Neva River estuary. The southern and northern boundaries of the basin were at 60° and 61° N, whereas western and eastern boundaries were at 19° and 30°40′ E, respectively. The western part of the southern boundary, approximately from the coast of Sweden to the Estonian coast, was open. This simulated the effect of the main part of the Baltic Sea on the dynamics of the processes modeled. The bottom relief was described by an analytical function, which approximates the characteristic features of the model area (Fig. 1). The maximum and minimum depths of the basin were 180 and 1 m, respectively.

The calculations were performed for two different (low and high) horizontal resolutions of the model. For the low resolution, the grid steps were h_λ = 5' with respect to the latitude and h_θ = 2.5' with respect to the longitude. For the high resolution, they were 5 times smaller and comprised h_λ = 1' and h_θ = 0.5'. In both cases, the vertical resolution was the same. Thirteen σ-levels

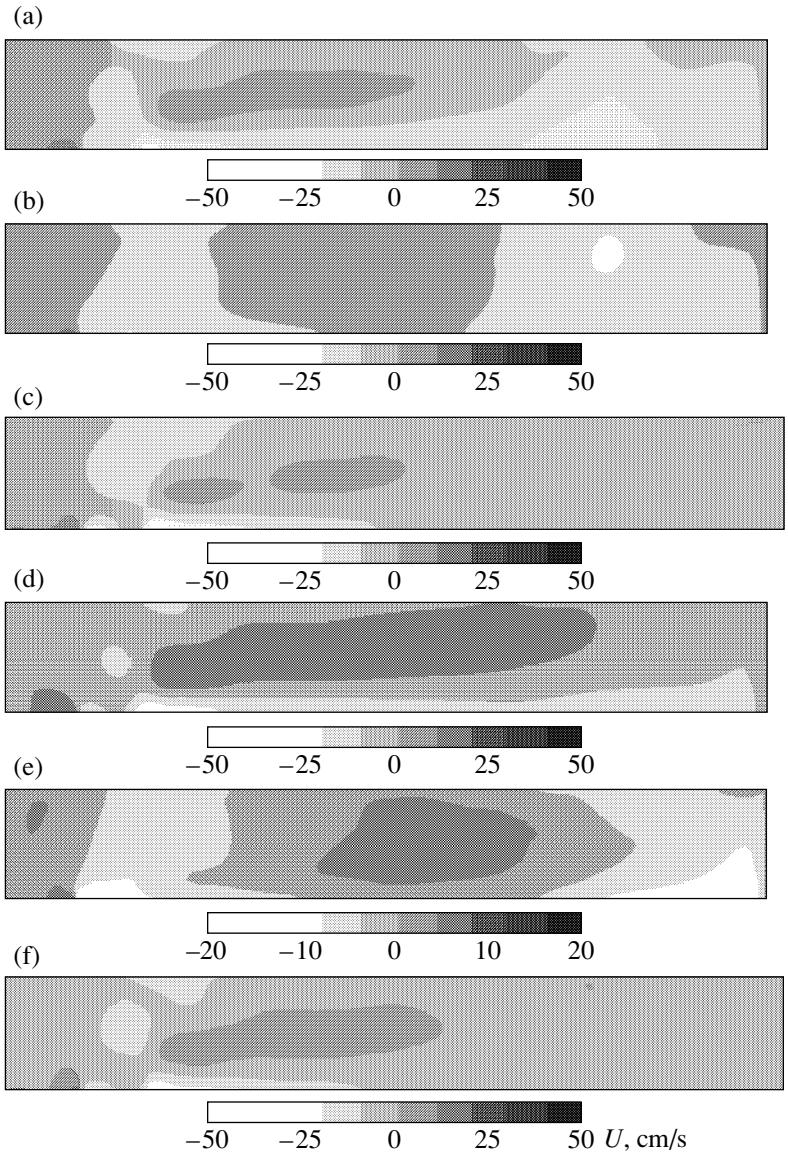

Fig. 4. U-component of the velocity at the 1st and 8th calculation levels in the academic basin on May 9, 1995, at 12:00 AM. (a) Surface, hydrostatic approximation, low resolution; (b) surface, nonhydrostatic approximation, low resolution; (c) surface, nonhydrostatic approximation, high resolution; (d) 8th calculation level, hydrostatic approximation, low resolution; (e) 8th calculation level, nonhydrostatic approximation, low resolution; and (f) 8th calculation level, nonhydrostatic approximation, high resolution.

were used, with their concentration toward the top boundary. The minimum vertical step (in terms of the z-system) varied from 1.8 m to 1 cm. The time step τ in the calculations for the hydrostatic and nonhydrostatic models was the same. Depending on the grid size, it was 30 min for the low resolution and 6 min for the high resolution.

The numerical experiment was carried out in the prognostic regime. At the initial moment of time, water motion is absent. The initial fields of temperature and salinity were given by analytical functions, which described the mean climatic spring distributions of the fields with the mixed upper layer. The calculations were performed for the time interval from April 30, 1995, to December 31, 1995. During the calculation period, the wind and heat conditions (the atmospheric wind and temperature) at the surface were set to be close to the actual ones, using the data of the calculations with the HIRLAM meteorological model [13]. The salinity flux at the surface throughout the calculation period was assumed to be zero.

We performed four calculations for the following conditions:

—hydrostatic model, low horizontal resolution;

—nonhydrostatic model, low horizontal resolution;

—nonhydrostatic model, high horizontal resolution;

—hydrostatic model, high horizontal resolution.

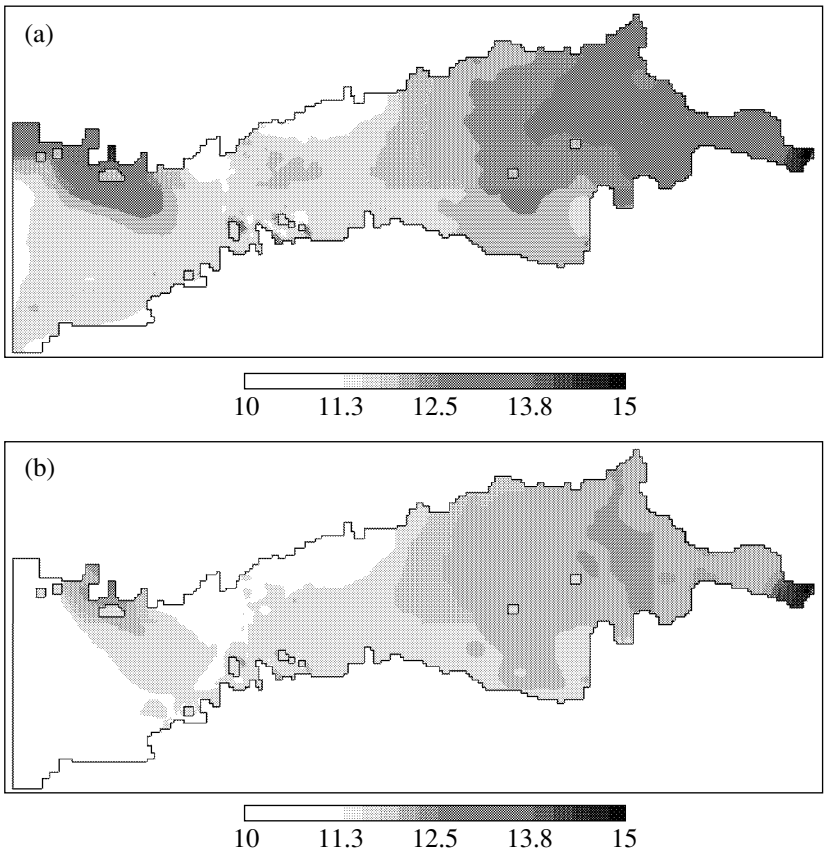

Fig. 5. Surface temperature in the Gulf of Finland on June 8, 1995, at 12:00 AM. (a) Nonhydrostatic model and (b) hydrostatic model.

The numerical experiment showed the numerical algorithm to be efficient for the calculation for all four model versions. The results obtained can be briefly described as follows.

—The model simulates the qualitative structure of the temperature and salinity fields characteristic of the summer conditions in the Gulf of Finland (Fig. 1).

—For the low horizontal resolution, the hydrostatic and nonhydrostatic models yield qualitatively and, to some extent, quantitatively close results.

—The differences in the solutions are mostly confined to the upper layer (temperature, Fig. 2; salinity, Fig. 3; and the *u*-component of the velocity, Fig. 3); they are most pronounced in the temperature field.

—In deeper layers, the calculated fields for all three versions differ insignificantly. The salinity in the lower layers is approximately the same for all the calculation versions, including the fourth variant.

—For the low spatial resolution, the solution of the hydrostatic model yields larger horizontal gradients in comparison to the solution of the nonhydrostatic model. The reason is that, in the nonhydrostatic case, we observe high vertical velocities and more intensive localized circulation cells which erode the horizontal gradients of the hydrological fields.

—The solution of the high-resolution nonhydrostatic model demonstrates an increase in the spatial gradients in comparison to the low-resolution nonhydrostatic model solution. Pronounced differences are inherent in the temperature field. The reason lies in the more intensive vertical velocity field. It should be noted that there are minimums in the field of the sea surface temperature (Fig. 2c). They are about 1°C in magnitude and concentrate near the northern boundary and in the western part of the basin. The sea surface temperature minimums are caused by upwelling processes. This feature is important from the point of view of the modeling of marine ecosystems. The numerical experiment shows that, in order to describe the dynamics of the upper layer in detail, it is necessary to use nonhydrostatic models with high resolution.

—The calculations with the hydrostatic model of high spatial resolution provide inadequately high values of the temperature in the upper layer. At the northwestern boundary, the values of the sea surface temperature reach 15°C in the first third of May.

NUMERICAL EXPERIMENT. GULF OF FINLAND

To approbate the model under actual conditions, we performed calculations of the dynamics of the Gulf of

Finland. The numerical experiment was carried out in the prognostic regime, completely similar to the previous case. The calculations were performed for the period from April 30, 1995, to October 18, 1995. At the surface of the basin, we set the actual wind friction stress and heat flux calculated from the HIRLAM forecast data [13]. As previously, the salinity flux was assumed to be zero.

Figures 5a and 5b show the calculated sea surface temperature fields for the nonhydrostatic and hydrostatic cases on June 8, 1995. A comparison of the calculated fields with the observation data reveals two essential points. First, over most of the area of the calculation domain, the model fields are close to each other and to the actual fields. Second, there are pronounced discrepancies in the vicinity of the western boundary, where, in the hydrostatic approximation, the calculated temperature is inadequately low.

The western boundary of the model was open. At this boundary, we set the distributions of the temperature and salinity characteristic for the summer season as the initial conditions. As can be seen from Fig. 5a, the nonhydrostatic model provides adequate results throughout the calculation domain, up to the periphery of the western contour. In the hydrostatic approximation, the temperature in the western subdomain is inadequately low, reaching values about 6°C, whereas the temperature observed in this period is close to that calculated with the nonhydrostatic model and equal to about 10–11°C.

Two essential points should be noted from the present numerical experiment: the nonhydrostatic model of the sea dynamics is adequate and has an advantage over the hydrostatic model in simulating the actual processes, in particular, with the open boundary. In the present study, we did not analyze in detail the reasons for the characteristic features of the solutions mentioned above, as this is beyond our objectives. It should only be noted that a possible reason for the reduced adequacy of the hydrostatic model in the experiment presented may be its higher sensitivity to the conditions at the liquid boundary. In the hydrostatic approximation, the vertical motion is more intensive, which decreases the area affected by the open boundary (in the horizontal plane); this results in the improvement of the model.

ACKNOWLEDGMENTS

This study was supported by the Russian Academy of Sciences, NIOKR no. 10002-251/P-14/197-020/140503-073.

REFERENCES

1. V. B. Zalesnyi and R. E. Tamsalu, *Numerical Analysis of Sea Dynamics* (IVM RAN, Moscow, 2000), pp. 110–124 [in Russian].
2. A. A. Kordzadze, *Mathematical Issues of the Solution of Ocean Dynamics Problems* (VTs SO AN SSSR, Novosibirsk, 1982) [in Russian].
3. G. I. Marchuk, "On Numerical Solution of the Poincare Problem for Oceanic Circulation," Dokl. Akad. Nauk SSSR **185** (5), 1041–1044 (1969).
4. G. I. Marchuk, *Splitting Methods* (Nauka, Moscow, 1988) [in Russian].
5. G. I. Marchuk, V. P. Dymnikov, and V. B. Zalesnyi, *Mathematical Models of Geophysical Hydrodynamics and Numerical Methods for Their Realization* (Gidrometeoizdat, Leningrad, 1987) [in Russian].
6. H. Burchard and H. Baumert, "On the Performance of a Mixed-Layer Model Based on the k–ε Turbulence Closure," J. Geoph. Res. **100** (C5), 8523–8540 (1995).
7. A. E. Gill, *Atmosphere–Ocean Dynamics* (Academic, New York, 1982).
8. S. M. Griffies, C. Boening, F. O. Bryan, *et al.*, "Developments in Ocean Climate Modeling," Ocean Modeling **2** (3–4), 123–192 (2000).
9. G. I. Marchuk and V. I. Kuzin, "On the Combination of the Finite Element and Splitting-Up Methods in the Solution of the Parabolic Equations," J. Comp. Phys. **52** (2), 237–272 (1982).
10. G. I. Marchuk, J. Siindermann, and V. B. Zalesny, "Mathematical Modeling of Marine and Oceanic Currents," Russ. J. Numer. Anal. Math. Modelling **16** (4), 331–362 (2001).
11. J. Marshall, C. Hill, L. Perelman, and A. Adcroft, "Hydrostatic, Quasi-Hydrostatic, and Nonhydrostatic Ocean Modeling," J. Geophys. Res. **102** (C3), 5733–5752 (1997).
12. J. Marshall, H. Jones, and C. Hill, "Efficient Ocean Modeling Using Non-Hydrostatic Algorithms," J. Marine Systems **18**, 115–134 (1998).
13. V. Perov, S. Zilitinkevich, and K.-I. Ivarsson, "Implementation of a New Parameterization of the Surface Turbulent Fluxes for the Stable Stratification in 3D HIRLAM," HIRLAM Newsletter, No. 38, 88–94 (2001).
14. A. S. Sarkisyan and V. B. Zalesny, "Splitting-up Method and Adjoint Equation Method in the Ocean Dynamics Problem," Russ. J. Numer. Anal. Math. Modelling **15** (3–4), 333–347 (2000).
15. V. B. Zalesny, "Numerical Simulation and Analysis of the Sensitivity of Large-Scale Ocean Dynamics," Rus. J. Numer. Anal. Math. Modelling **11** (6), 421–443 (1996).